Supplement of Biogeosciences, 14, 5217–5237, 2017
https://doi.org/10.5194/bg-14-5217-2017-supplement
© Author(s) 2017. This work is distributed under
the Creative Commons Attribution 3.0 License.

Biogeosciences Open Access EGU

Supplement of

Carbon uptake and biogeochemical change in the Southern Ocean, south of Tasmania

Paula Conde Pardo et al.

Correspondence to: Paula C. Pardo (paula.condepardo@csiro.au)

The copyright of individual parts of the supplement might differ from the CC BY 3.0 License.

Supplementary material

S.1 Biogeochemical Model.

The 1/10° biogeochemical ocean simulation is based on the near-global Ocean Forecasting Australia Model configuration (OFAM3) (Oke et al., 2013) with 51 vertical layers (14 layers between the surface and 100 m depth and partial cells to better represent bottom topography), a resolution of 4.7km at 65°S, 7.8km at 45°S and a constant meridional resolution of 11 km. This configuration represents the frontal structure and filament nature of the ACC and captures much of the mesoscale variability and the development of baroclinic eddies (Langlais et al., 2011, 2015). OFAM3 includes the World Ocean Model of Biogeochemistry and Trophic dynamics (WOMBAT) (Kidston et al., 2011; Oke et al., 2013) that is based on a nutrient, phytoplankton, zooplankton and detritus model, with the addition of an O_2 and CO_2 cycle. The ocean model is based on the version 4p1d of the Geophysical fluid Dynamics Laboratory Modular Ocean Model (Griffies, 2009). Horizontal mixing is provided by the biharmonic Smagorinsky viscosity scheme (Griffies and Hallberg 2000), and vertical mixing by the K-profile parameterization (KPP, Large et al. 1994). It has two tracers of DIC, one that sees an (pre-industrial) atmospheric value of 280 ppm (natural carbon tracer), and a second tracer that sees the observed rising atmospheric pCO_2 (total carbon tracer). The BGC parameters used with WOMBAT are based on Oschlies and Schartau (2005), with extra parameters for the carbon cycle (Law et al., 2017).

The 1/10° simulation spans from 1979 to 2014, forced by 3-hourly Japanese 55-year Reanalysis (JRA-55; Kobayashi et al., 2015), using bulk formula (Large and Yeager, 2004) for wind stress, turbulent sensible and latent fluxes, and evaporation. As the model is not coupled to a sea-ice model, the effects of sea-ice on heat and freshwater fluxes are accounted for by the use of the JRA-55 sea ice coverage field to mask the applied atmospheric fields. Below 2000m, a non-adaptive relaxation keeps the deep-ocean close to the observed climatology but allows the climate changes signals to penetrate to the deep ocean.

The model BGC fields are initialised with fields constructed from observations. Specifically, the World Ocean Atlas is used to initialise nutrients (phosphorus) and oxygen (Garcia et al 2006a; Garcia et al. 2006b). The Global Ocean Data Analysis Project (GLODAP) is used to initialise alkalinity and dissolved carbon (Sabine et al. 2004; Key et al. 2004). Phytoplankton is initialised with SeaWIFS observation (NASA, 2014) and zooplankton is initialised as a fraction of phytoplankton (0.05). As the inclusion of the BGC component is computationally expensive, the BGC fields are only integrated between 1992 and 2014. This duration spans the era of relevant satellite sea-colour observations.

S.2 OMP analysis.

The OMP method (Thompson and Edwards, 1981; Tomczak, 1981; Mackas et al., 1987; Tomczak and Large, 1989) considers the water samples as nodes of a grid in which the different properties (e.g., S, θ, O_2) are measured. The OMP assumes that the value of each property is the result of the linear mixing of the water masses characterizing the region of study, which are called end members or source water types (SWT) and whose characteristics are known. Thus, the value of each node can be expressed as a linear combination of the SWTs:

$$P_i = \sum_{j}^{Nj} \left(SWT_j * P_j + R_i * \Delta O_2 \right)$$

where P_i is the value of the properite i in the node, P_j is the value of the correspondent properties of the j SWT. Since some of the measured variables are non-conservative (e.g., O_2), biogeochemical terms have to be included in the mixing equations ($R_i * \Delta O_2$) that are based on Redfield ratios and considered constant (R_i, Broecker, 1974; Anderson and Sarmiento 1994; Martiny et al., 2013). Here we use R_N=9 and R_P = 125, referenced to the oxygen consumption (~ΔO_2) which were the optima after a sensibility analysis (Álvarez et al., 2014). SiO_4 is considered a conservative variable (see sensitivity analysis in section 6.4). These stoichiometric ratios are in agreement with previous studies (Le Jehan and Treguer, 1983; Verlencar et al., 1990; Lourey and Trull, 2001, see section 4.4.2).

The system of equations (resulting from considering all the properties measured in each sample plus a mass balance equation) is normalized and solved by a least square method with a positive definite constraint to obtain the fractions of each of the SWTs characterizing the water sample and satisfying the mass balance equation.

Before solving the system, each equation is weighted (the mass equation presents the highest weight to ensure its conservation) based on the accuracy of the property and/or the variability in the region of study (Table S1). Weights were also adjusted so that the ratios between the Standard Deviations of the Residuals and the analytical error (ε, Table S1) were almost the same for all the SWT properties (Table S1).

Here we consider 11 SWTs that characterize the water masses of the SR03 section, i.e., those that best enclose the main features of the T/S diagram and of other properties of the water masses of the section (Fig. S1). The conservative properties (θ and S) were defined based on bibliography available (Table S1):

- In order to take into account the subtropical waters two points were defined as upper limits in the T/S diagram (Fig. S1). These end members correspond to the main properties of both the Zeehan Current (ZC) and the EAC arriving to the north part of the section (Fig. 1). The end member SWT_{STW15} represents the extension of the ZC (~15°C, ~35) in winter to the region south of Tasmania described by Cresswell (2000). The reference for the characterization of the subtropical waters from the EAC, i.e., SWT_{STW16}, is the southern component of the Subtropical Lower Water, characterized by Sokolov and Rintoul (2000) as waters in the range 16-22°C and 35.5-35.7. These two end members are considered together for the study as $SWT_{STW} = SWT_{STW16} + SWT_{STW15}$.
- Two end members are used to represent the seasonal warming of the AASW as it extends from the Antarctic shelf to latitudes of the SAF. SWT_{AASW} is the AASW described by Mosby (1934) and defined by Pardo et al. (2012). SWT_{SASW} represents the warmest type of AASW found in summer based on Chaigneau et al. (2004). In our study, the two endmembers are considered together as $SWT_{AAS} = SWT_{AASW} + SWT_{SASW}$, as is the case of subtropical waters.
- HSSW is produced in coastal polynyas, where ice-formation creates salty surface waters (Orsi et al., 2002). This water is also the precursor in the formation of bottom waters. The definition of the end member SWT_{HSSW} was obtained from the study of Lacarra et al. (2011) within the Adélie -George V Land coast (Fig. 1), one of the areas of formation of ALBW.
- SWT_{SAMW} represents the core of the SAMW that is ventilated south of Tasmania (Rintoul and Bullister, 1999). We defined this end member as a point inside the cluster defined by Herraiz-Borreguero and Rintoul (2010) (8.5-9°C, 34.58-34.68).
- The end member characterizing AAIW, SWT_{AAIW}, is the variety of AAIW found south of Tasmania and close to the SAF and is defined by T of 4-4.5°C and S of 34.35 after Rintoul and Bullister, (1999).

- SWT_{NADW} reflects the properties of the NADW in South Atlantic, when it arrives to the ACC and is defined by Pardo et al. (2012).
- The end member SWT_{CDW} refers to waters in the deep bottom layers of the ACC that result from the mix with NADW arriving to the ACC, AAIW from above and the upper layers of the AABW, which, in specific locations of the Antarctic continent contributes to the formation of bottom waters. The properties of this end member are taken from Pardo et al. (2012).
- The end member SWT_{PIDW} refers to waters in the deep layers of the ACC (known as Lower Circumpolar Deep water) that are fed by deep waters from the Pacific and Indian Oceans and are characterized by a silicate maximum, high nutrients and low oxygen (e.g., Callahan, 1972; Whitworth et al., 1998). The values from the SWT_{PIDW} were obtained from Talley et al. (2011).
- SWT_{AABW} is the end member representing the bottom waters in the southern end of the section, close to the Antarctic shelf that result from a mixing between recently formed ALBW and RSBW. The definition of this end member is based on the observations from Rintoul and Bullister (1999).

The values of the non-conservative variables of the SWTs were initially extrapolated from regression lines with salinity and temperature (Poole and Tomczak, 1999) and then subjected to an iterative process in OMP in order to obtain the types that best fit the cruise data.

The number of SWTs included in the mixing depends on the number of properties measured at the node. In order to have enough degrees of freedom to solve the system of equations, we use combinations of water masses that we call mixing groups (Table S2), to solve different regions of the section. Each mixing group is connected to the other by one or more SWTs in order to maintain the continuity of the analysis (Fig. S1), and are defined by considering the vertical characteristics and/or dynamics of the water masses in the region of study.

The robustness of the OMP analysis is tested through a perturbation analysis of uncertainties (Lawson and Hanson, 1974). The properties of both each SWT and each water sample are perturbed in order to check the sensitivity of the model to variations in the SWTs, due to environmental variability, and in the water samples, due to measurement errors (Leffaune and Tomczak, 2004). The uncertainties of the SWTs fractions (mean standard deviation of 100 perturbation runs) are shown together with the percentage of variability explained by the OMP analysis for each variable (Table S1). The model is reliable since it explains at least 98% of the variability of all the variables implicated (Table S1).

S.3 Parameterizations of TA^0 and CDIS.

The values of TA^0 and CDIS are defined for each SWT (Table S1) using the parameterizations and values from Pardo et al. (2011) and Pardo et al. (2014) (Table S3). Since mode and intermediate waters (SWT_{SAMW} and SWT_{AAIW}, Table S3) are formed and ventilated in areas influenced by subtropical waters and Antarctic waters, we combine the parameterizations for subtropical ([1]) and Antarctic ([2]) regions to obtain better values of both parameters (Table S3). The values of TA^0 and CDIS for the SWTS of mode and intermediate waters are estimated as $TA^0 = \frac{2}{3}(TA^0[1]) + \frac{1}{3}(TA^0[2])$ and $CDIS = \frac{2}{3}(CDIS[1]) + \frac{1}{3}(CDIS[2])$ (Table S2). The values obtain for TA^0 and CDIS for each SWT are then extended to the water column using the results from the OMP analysis:

$$TA^0 = \sum_{j=1}^{11}\left(SWT_j * TA_j^0\right); \quad CDIS = \sum_{j=1}^{11}\left(SWT_j * CDIS\right)$$

The appropriate combination of the parameterizations of TA^0 for the section is obtained by analysing the differences between TA and TA^0 at surface layers of the section, once TA^0 is determined by OMP analysis in order to avoid negative values. The values obtained for CDIS were very similar for all the SWTs except for SWT_{HSSW}, with an estimated CDIS value 4 times bigger than that some of the SWTs. Since the results from Landschutzer et al. (2015) indicate that the disequilibrium values do not change much between AASW and SAMW, we considered the value of CDIS obtained from the monthly mean values of atmospheric CO_2 from the NOAA network (1968-2015, Dlugokencky, et al., 2016) for latitudes > 62°S, as the most appropriate for SWT_{HSSW}.

For the SWT_{NADW}, the value of TA^0 are obtained from the GLODAPv2 climatology (http://cdiac.ornl.gov/oceans/GLODAPv2; Lauvset et al., 2016) in the area of the Indian Ocean and that of CDIS from Pardo et al. (2014). The SWTs for the rest of deep and bottom waters are formed by mixing of other water masses and the values of TA^0 and CDIS are obtained through an iterative process considering the composition of each SWT (Table S3) obtained from temperature and salinity. In the iterative process a default value is given to TA^0 and CDIS of SWT_{AABW} and iterations are run for the different deep-bottom water masses until the differences between the values of TA^0 and CDIS of two consecutive iterations are less than 0.005 for TA^0 and 0.05 for CDIS.

References.

Álvarez, M., Brea, S., Mercier, H. and Álvarez-Salgado, X.A.: Mineralization of biogenic materials in the water masses of the South Atlantic Ocean. I: assessment and results of an optimum multiparameter analysis, Progress in Oceanography, 123, 1-23, doi: 10.1016/j.pocean.2013.12.007, 2014.

Anderson, L.A. and Sarmiento, J.L.: Redfield ratios of remineralization determined by nutrient data analysis. Global Biogeochemical Cycles 8 (1), 65–80, doi: 10.1029/93GB03318, 1994.

Broecker, W.S.: "NO" a conservative water mass tracer. Earth and Planetary Science Letters 23, 8761–8776, 1974.

Callahan, J.E.: The structure and circulation of Deep Water in the Antarctic, Deep-Sea Research, 19, 563-575, 1972.

Chaigneau, A., Morrow, R.A. and Rintoul, S.R.: Seasonal and interannual evolution of the mixed layer in the Antarctic Zone south of Tasmania, Deep-Sea Research I, 51, 2047–2072, doi:10.1016/j.dsr.2004.06.013, 2004.

Cresswell, G.: Currents of the continental shelf and upper slope of Tasmania, In Banks, M.R. & Brown, M.j. (Eds): Tasmania and the Southern Ocean, Pap. Proc. R. Soc. Tasm., 133, 3, 21-30, 2000.

Dlugokencky, E.J., Lang, P.M., Mund, J.W., Crotwell, A.M., Crotwell, M.J. and Thoning, K.W.: Atmospheric Carbon Dioxide Dry Air Mole Fractions from the NOAA ESRL Carbon Cycle Cooperative Global Air Sampling Network, 1968-2015, Version: 2016-08-30,ftp://aftp.cmdl.noaa.gov/data/trace_gases/co2/flask/surface/, 2016.

Garcia, H.E., Locarnini, R.A., Boyer, T.P. and Antonov, J.I.: World ocean atlas 2005, volume 3: dissolved oxygen, apparent oxygen utilization, and oxygen saturation, In: Levitus, S. (Ed.), NOAA Atlas NESDIS 63. U.S. Government Printing Office, Washington, D.C., p. 342, 2006a.

Garcia, H.E., Locarnini, R.A., Boyer, T.P. and Antonov, J.I.: World ocean atlas 2005, volume 4: nutrients (phosphate, nitrate, silicate). In: Levitus, S. (Ed.), NOAA Atlas NESDIS 64. U.S. Government Printing Office, Washington, D.C., p. 396, 2006b.

Griffies, SM., et al.: Coordinated Ocean-Ice Reference Experiments (COREs), Ocean Modell., 26, 1–46, doi:10.1016/j.ocemod.2008.08.007, 2009.

Griffies, S.M. and Hallberg, R.W.: Biharmonic friction with a Smagorinsky viscosity for use in large-scale eddy permitting ocean models, Mon. Weather Rev. 128, 2935–2946, 2000.

Herraiz-Borreguero, L. and Rintoul, S.R.,: Subantarctic mode water variability influenced by mesoscale eddies south of Tasmania. J. Geophys. Res. 115, C04004, doi:10/1029/2008JC005146, 2010.

Key, R.M., et al.: A global ocean carbon climatology: Results from Global Data Analysis Project (GLODAP), Global Biogeochem. Cycles, 18, GB4031, doi:10.1029/2004GB002247, 2004.

Kidston, M., Matear, R. J. and Baird, M. E.: Parameter optimisation of a marine ecosystem model at two contrasting stations in the Sub-Antarctic Zone, Deep-Sea Res., 58, 2301–2315, 2011.

Kobayashi, S., et al.: The JRA-55 Reanalysis: General specifications and basic characteristics. J. Meteor. Soc. Japan, 93, 5-48, doi:10.2151/jmsj.2015-001, 2015.

Lacarra, M., et al.: Summer hydrography on the shelf off Terre Ade´lie/George V Land based on the ALBION and CEAMARC observations during the IPY, Polar Science, 5, 2011, 88-103, doi:10.1016/j.polar.2011.04.008, 2011.

Landschützer, P., et al.: The reinvigoration of the SouthernOcean carbon sink, Science, 349, 1221–1224, doi:10.1126/science.aab2620, 2015.

Langlais, C., Rintoul, S. and Schiller, A.: Variability and mesoscale activity of the Southern Ocean fronts: Identification of a circumpolar coordinate system, doi:10.1016/j.ocemod.2011.04.010, Ocean Modelling, 39, 79–96, 2011.

Langlais, C.E., Rintoul, S.R. and Zika, J.D.: Sensitivity of Antarctic Circumpolar Current Transport and Eddy Activity to Wind Patterns in the Southern Ocean, Journal of Physical Oceanography, 45, 1051-1067, doi:10.1175/JPO-D-14-0053.1, 2015.

Large, W. G., McWilliams, J.C. and Doney, S.C.: Oceanic vertical mixing: a review and a model with a nonlocal boundary layer parameterization. Rev. Geophys., 32, 363-403, 1994.

Large, W.G. and Yeager, S.G.: Diurnal to decadal global forcing for ocean and sea-ice models: the data sets and flux climatologies, TN-460+STR, NCAR technical note, 111 pp, doi: 10.5065/D6KK98Q6, 2004.

Lauvset, S. K, et al.: A new global interior ocean mapped climatology: the 1°x1° GLODAP version 2, Earth Syst. Sci. Data, 8, 325–340, doi:10.5194/essd-8-325-2016, 2016.

Lawson, C.L. and Hanson, R.J.: Solving Least Squares Problems, Prentice-Hall, Englewood Cliffs, NJ., 1974.

Law, R. M. et al.: The carbon cycle in the Australian Community limate and Earth System Simulator (ACCESS-ESM1) Part 1: Model description and pre-industrial simulation, Geosci. Model Dev., 10, 2567–2590, https://doi.org/10.5194/gmd-10-2567-2017, 2017.

Leffaune H. and Tomczak M.: Using OMP analysis to observe temporal variability in water mass distribution, J. Mar. Syst, 48, 3–14, 2004.

Le Jehan, S. and Treguer, P.: Uptake and regeneration ASi/AN/AP ratios in the Indian Sector of the Southern Ocean. Polar Biol. 2: 127-136, 1983.

Lourey, K.J. and Trull, T.W.: Seasonal nutrient depletion and carbon export in the Subantarctic and Polar Frontal Zones of the Southern Ocean south of Australia, J. Geophys. Res., 106, C12, 31,463-31,487, 2001.

Mackas, D.L., Denman, K.L. and Bennett, A.F.: Least squares multiple tracer analysis of water mass composition, Journal of Geophysical Research ,92, C3, 2907–2918, doi: 10.1029/JC092iC03p02907, 1987.

Martiny, A.C., et al.: Strong latitudinal patterns in the elemental ratios of marine plankton and organic matter, Nature, 6, 279-283, doi: 10.1038/NGEO1757, 2013.

Mosby, H.: The waters of the Atlantic Antarctic Ocean, Scientific Results of the Norwegian Antarctic Expeditions 1927-1928, 1, 11, 131 pp, 1934.

Oke, P.R., et al.: Evaluation of a near-global eddy-resolving ocean model, Geosci. Model Dev., 6, 591–615, doi:10.5194/gmd-6-591-2013, 2013.

Orsi, A.H., Smethie Jr., W.M. and Bullister, J.L.: On the total input of Antarctic waters to the deep ocean: A preliminary estimate from chlorofluorocarbon measurements, J. Geophys. Res., 107, C8, 3122, doi: 10.1029/2001JC000976, 2002.

Oschlies A. and Schartau, M.: Basin-scale performance of a locally optimized marine ecosystem model, Journal of Marine Research, 63, 2, 335-358, 2005.

Pardo, P.C., Vázquez-Rodríguez, M., Pérez, F.F. and Ríos, A.F.: CO_2 air-sea disequilibrium and preformed alkalinity in the Pacific and Indian Oceans calculated from subsurface layer data, Journal of Marine Systems 84, 67–77, doi:10.1016/j.jmarsys.2010.08.006, 2011.

Pardo, P.C., Perez, F.F., Velo, A. and Gilcoto, M.: Water masses distribution in the Southern Ocean: improvement of an extended OMP (eOMP) analysis. Progress in Oceanography 103, 92–105, doi: 10.1016/j.pocean.2012.06.00, 2012.

Pardo, P.C., Pérez, F.F., Khatiwala, S. and Ríos, A.F.: Anthropogenic CO_2 estimates in the Southern Ocean: Storage partitioning in the different water masses, Progress in Oceanography, 120, 230–242, doi:10.1016/j.pocean.2013.09.005, 2014.

Poole, R. and Tomczak, M.: Optimum multiparameter analysis of the water mass structure in the Atlantic Ocean thermocline, Deep Sea Res., Part I, 46, 1895– 1921, doi:10.1016/S0967-0637(99)00025-4, 1999.

Rintoul, S.R. and Bullister, J.L.: A late winter hydrographic section from Tasmania to Antarctica, Deep –Sea Research I, 46, 1417-1454, 1999.

Sabine, C.L., et al.: The Oceanic Sink for Anthropogenic CO_2, Science, 305, 5682, 367–371, 2004.

Sokolov, S. and Rintoul, S.R.: Circulation and water masses of the southwest Pacific: WOCE Section P11, Papua New Guinea to Tasmania, Journal of Marine Research, 58, 223–268, 2000.

Talley, L.D., Pickard, G.L., Emery, W.J. and Swift, J.H.: Descriptive Physical Oceanography: An Introduction (Sixth Edition), Elsevier, Boston, 560 pp, 2011.

Thompson, R.O. and Edwards, R.J., 1981. Mixing and water-mass formation in the Australian Subantarctic. Journal of Physical Oceanography 11, 1399–1406, 1981.

Tomczak, M.: A multi-parameter extension of temperature/salinity diagram techniques for the analysis of non-isopycnal mixing, Progress in Oceanography, 10, 147–171, 1981.

Tomczak, M. and Large, D.G.B.: Optimum Multiparameter Analysis of Mixing in the Thermocline of the Eastern Indian Ocean Journal of Geophysical Research, 94, Cll, 16141-16149, 1989.

Verlencar, X.N., Somasunder, K. and Qasim, S.Z.: Regeneration of nutrients and biological productivity in Antarctic waters, Marine Ecology Progress Series, 61, 41-59, 1990.

Whitworth III, T., Orsi, A.H., Kim, S.-J. and Nowlin, W.D.: Water masses and mixing near the Antarctic Slope Front. Antarctic Research Series, 75, 1–27, 1998.

D Figures & Tables Appendix

	θ (°C)	S	SiO_4 (µmol/kg)	NO_3^0 (µmol/kg)	PO_4^0 (µmol/kg)	O_2^{0*} (µmol/kg)	TA^0 (µmol/kg)	DIC^n_{SAT} (µmol/kg)	CDIS (µmol/kg)	$CDIS^n$ (µmol/kg)	Fractions uncertainties (%)
SWT_{STW16}	16 ± 0.06	35.1 ± 0.07	0.9 ± 0.2	1.2 ± 0.2	0.04 ± 0.3	243 ± 2	2290	1990	-19	1	0.04
SWT_{STW15}	15 ± 0.06	35.66 ± 0.07	0.6 ± 0.2	0 ± 0.2	0.12 ± 0.3	247 ± 2	2328	2026	-22	-2	0.04
SWT_{AASW}	-1.85 ± 0.006	33.8 ± 0.005	45 ± 2	30.7 ± 0.2	2.10 ± 0.3	360 ± 4	2289	2137	-23	-19	0.06
SWT_{SASW}	5 ± 0.008	33.8 ± 0.03	3 ± 0.2	23.3 ± 0.3	1.55 ± 0.5	310 ± 3	2264	2064	-13	-4	0.06
SWT_{HSSW}	-1.91 ± 0.08	34.71 ± 0.006	80 ± 1	28.3 ± 0.08	2.02 ± 0.03	300 ± 3	2351	2188	-21	0	0.08
SWT_{SAMW}	8.8 ± 0.02	34.63 ± 0.03	6 ± 0.6	13.2 ± 0.6	0.92 ± 0.8	280 ± 7	2290	2053	-10	2	0.03
SWT_{AAIW}	4 ± 0.01	34.35 ± 0.02	34 ± 2	29.2 ± 0.4	1.97 ± 0.9	220 ± 8	2299	2099	-16	-6	0.04
SWT_{NADW}	3.28 ± 0.008	34.91 ± 0.003	28 ± 1	27.5 ± 0.3	1.19 ± 0.7	220 ± 4	2355	2152	-27	-10	0.08
SWT_{CDW}	0.65 ± 0.006	34.707 ± 0.003	115 ± 7	30.8 ± 0.1	2.12 ± 0.1	220 ± 3	2351	2168	-23	-2	0.03
SWT_{PIDW}	1.44 ± 0.008	34.75 ± 0.005	125 ± 3	34.2 ± 0.01	3.4 ± 0.02	96 ± 2	2360	2168	-24	-4	0.04
SWT_{AABW}	-0.6 ± 0.006	34.66 ± 0.006	130 ± 5	30.7 ± 0.08	2.13 ± 0.03	259 ± 3	2355	2181	-22	-2	0.05
Weights	20	10	0.5	1	1	1					
SDR	0.004	0.003	6.0	0.50	0.04	2.0					
r^2	0.99	0.99	0.98	0.99	0.99	0.99					

Table S1. Properties of the SWTs characterizing the water masses of the SR03 section with the correspondent accuracies (ε). All SWTs are defined with preformed values of the variables (°). *The values of preformed oxygen (O_2°) are not in equilibrium for end members representing waters from the Antarctic shelf or old deep waters. The uncertainties in the fractions of the SWTS, the weights given to each variable in the OMP analysis, the Standard Deviation of the Residuals (SDR) and the square correlation coefficient (r^2) between the observed values and the OMP estimates are also listed.

Mixing Groups
STW15 + SAMW + SASW + STW16
SASW + SAMW + AAIW + AASW
SAMW + AAIW + NADW
AAIW + PIDW + NADW
AASW + AAIW + CDW
CDW + AABW + HSSW + AASW

Table S2. Mixing groups used in the OMP analysis. Note that only the subscripts of the names of the SWTs are written, i.e., STW15 instead of SWT_{STW15}.

Table S3. Parameterizations for estimating AT^0 and CDIS in each of the SWTs. PO =R_PPO_4 + O_2. For SWT_{HSSW} *, CDIS is obtained from the NOAA database of latitudinal mean values of atmospheric CO_2. For SWT_{NADW}, AT^0 is obtained from the climatology of GLODAPv2 and CDIS from Pardo et al. (2014).**

SWTs	Parameterizations	Reference
SWT_{STW16}	**AT°** (±6) = 2288.3 + 62.8*(S - 35) - 0.9*(θ -16) + 0.1*(PO - 300) **CDIS** (±5) = -47.9 + 2.31*θ + 0.16*(PO - 300)	Parameterizations for the South Subtropical region-Pacific Ocean (SSTIP, Pardo et al., 2011)
SWT_{STW15}	**AT°** (±6) = 2288.3 + 62.8*(S - 35) - 1.6*(θ -16) + 0.1*(PO - 300) **CDIS** (±5) = 51.3 + 2.31*θ + 0.16*(PO - 300)	Parameterizations for the South Subtropical region-Indian Ocean (SSTIP, Pardo et al., 2011)
SWT_{HSSW}* SWT_{AASW} $SWTS_{SASW}$	**AT°** (±4) = 2296.7 + 94.7*(S - 35) + 0.3*(PO - 300) **CDIS** (±5) = −84.3 − 12.95*(S - 35) + 5.75*θ + 0.17*(PO - 300)	Parameterizations for the Antarctic region (AAIP, Pardo et al., 2011) *(Dlugokencky, et al., 2016)
SWT_{SAMW} SWT_{AAIW}	**AT°[1]** (±6) = 2288.3 + 62.8*(S - 35) -(0.9//1.6)*(θ - 16) + 0.1*(PO - 300) **AT°[2]** (±4) = 2296.7 + 94.7*(S - 35) + 0.3*(PO - 300) **CDIS[1]** (±5) = -47.9 + 2.31*θ + 0.16*(PO - 300) **CDIS[2]** (±5) = −84.3 − 12.95*(S - 35) + 5.75*θ + 0.17*(PO - 300)	Parameterizations for the South Subtropical regions and for the Antarctic region (SSTIP, Pardo et al., 2011)
SWT_{NADW}	----------	GLODAPv2 // Pardo et al. (2014) **
SWT_{CDW}	**AT° // CDIS** = 0.69*(AT° // CDIS)$_{AABW}$ + 0.26*(AT° // CDIS)$_{NADW}$ + 0.05*(AT° // CDIS)$_{AAIW}$	----------
SWT_{PIDW}	**AT° // CDIS** = 0.71*(AT° // CDIS)$_{CDW}$ + 0.25*(AT° // CDIS)$_{NADW}$ + 0.04*(AT° // CDIS)$_{AAIW}$	----------
SWT_{AABW}	**AT° // CDIS** = 0.51*(AT° // CDIS)$_{CDW}$ + 0.44*(AT° // CDIS)$_{HSSW}$ + 0.05*(AT° // CDIS)$_{AASW}$	----------

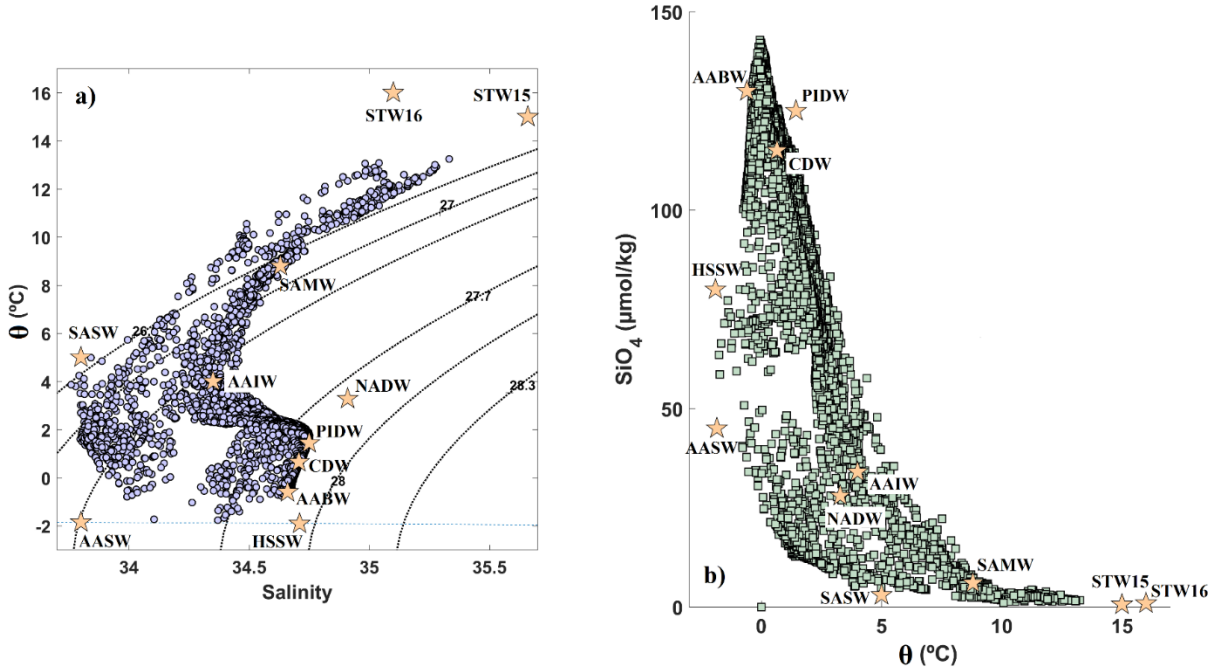

Fig. S1. (a) T/S diagram, with θ = potential temperature. Blue dots represent the data from all cruises for the period 1995-2011. Dotted lines indicate density (σ_0, kg m^{-3}). (b) SiO_4/T diagram, with θ = potential temperature. Green squares represent the data from all cruises for the period 1995-2011. Pentagrams represents the SWTs included in the OMP analysis (only subscripts are written, i.e., AASW instead of SWT_{AASW}).

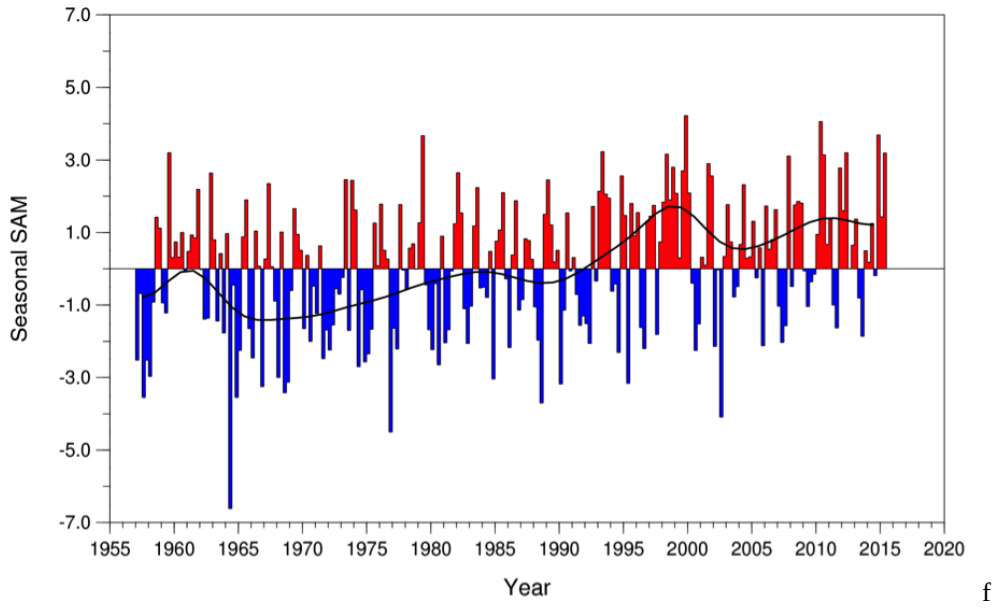

f

Fig. S2. Seasonal values of the observation-based SAM index. The smooth black curve shows decadal variations. Figure obtained from Marshall, Gareth & National Center for Atmospheric Research Staff (Eds). "The Climate Data Guide: Marshall Southern Annular Mode (SAM) Index (Station-based)." Retrieved from https://climatedataguide.ucar.edu/climate-data/marshall-southern-annular-mode-sam-index-station-based.